On-Orbit System Identification and Attitude Control Experiment of ETS-VI*

Keiji KOMATSU*1, Takashi KIDA*2, Masa-aki SANO*1,
Isao YAMAGUCHI*3, Tokio KASAI*1, Takashi SUZUKI*4, Shin-ichi ISHIKAWA*4,
Takeshi SEKIGUCHI*4, Syunsuke TANAKA*4, and Shin-ichiro ICHIKAWA*4

Abstract

This report describes the results od an on-orbit attitude and vibration control experiment of flexible spacecraft ETS-VI (Engineering Test Satelite-VI). The methods of pre-launch modeling, on-orbit model parameter identification and controller synthesis are outlined and the experiment results are discussed.

Keywords : spacecraft, vibration control, system identification, model analysis

概　　要

技術試験衛星VI型を使って軌道上での加振実験と制御実験を行った。軌道上実験に先立ち，一体構造としてモード試験のできない構造に対してモード合成法を使って動特性を推定した後，軌道上での加振実験を行い，さまざまな方法でデータ処理を行ってモード特性を同定し，地上でのモデリングの精度を検証した。これらの同定結果に基づいて６種の制御系を設計し，制御実験を行った。

1. INTRODUCTION

During the past two decades, the issues of modeling and control of large space structures have been studied extensively. Besides theoretical works, many experimental results have been reported. However, very few papers have appeared discussing on-orbit experimental results using actual spacecraft or large space structures, despite their obvious importance. Exceptions are the vibration test of Hermes[1], the Solar Array Flight Experiment (SAFE) [2], the Middeck Active Control Experiment (MACE) by the Space Shuttle[3] and the Hubble Space Telescope (HST) pointing control study [4].

With this motivation, we have been developing since 1987 an on-orbit dynamics and control experiment using Engineering Test Satellite VI (ETS-VI). This FLEXible structure modeling and control project (named FLEX) was successfully completed in 1995. The ETS-VI is a three-axis stabilized geo-synchronous satellite whose main mission is an advanced communication experiments. A view of the ETS-VI is shown in Fig.1. The body measures 30m×9.3m×7.8m and its initial weight in orbit was about 2000 kg. It has a pair of large, flexible, and light-weight solar array paddles, each paddle being 14m in length and 72 kg in weight.

Controlling such a large flexible spacecraft with high accuracy requires suppression of its structural vibration. Structural vibration control, however, is a challenging problem for the following reasons. First, the structural vibration is described by a high-order

＊　平成９年４月15日受付（received 15, April,1997）
＊１　構造力学部（Structural Mechanics Division）
＊２　電気通信大学，元宇宙研究グループ（University of Electro-Communications, former Space Technology Research Group）
＊３　制御部（Contorol System Division）
＊４　宇宙開発事業団（National Space Development Agency of Japan）

Fig. 1 ETS-VI on-orbit configuration

modal equation which mathematically has an infinite number of modes spread over a wide frequency-range. Second, accurate modal parameter identifi-cation is difficult in a 1-G ground environment. Third, the modal damping ratio is very small. Hence, in the worst case, light damping modes are easily excited by the controller, resulting in spillover destabilization of the closed-loop system. One way to overcome these problems is to construct a reduced-order model based on an accurately identified full-order model and to design a reduced-order controller which is robust against the inevitable model uncertainties.

In standard spacecraft development procedure, the controller is designed based on a model estimated before launch, and its computer code is loaded into the onboard computer memory. The designer does not know the fidelity of the pre-launch model during the design phase, neither, does he have any chance to retune the controller parameters after launch. Therefore, the accuracy of the pre-launch model is the most important problem for the success of the spacecraft mission, and the question" How robust is the controller ? " is not fully answered before launch. Through on-orbit experiments, we intended to experience the technology issues as a case study. To this end, we performed the following.

Prior to launch, the modal parameters of the satellite were estimated on the ground. A component mode synthesis method using measured modal data was applied to the flexible solar array paddle. Once in orbit, the satellite was excited by its Reaction Control System (RCS), and its modal parameters were identified based on attitude telemetry data from the Attitude Control System (ACS) and six Paddle Accelerometers (PACC). The attitude controllers were designed based on the pre-launch model and executed in orbit, and some controllers were re-tuned based on the on-orbit identification model.

This report is the English summary of the three NAL-NASDA joint research reports [5)6)7)] written in Japanese, which have been distributed locally.

2. PRE-FLIGHT MODAL PARAMETER IDENTIFICATION

As the spacecraft scale is growing larger to meet the mission requirements, it becomes harder to get accurate modal parameters on the ground test before launch because of the 1-G gravity and atmospheric environment. ETS-VI has a pair of large flexible solar array paddles and pre-launch vibration test in fully

deployed configuration was considered impossible, therefore, an alternative approach to verify the initial Finite Element Method (FEM) model, namely component mode synthesis using measured modal data was developed.

The component mode synthesis technique is well established in the field of purely computational finite element analysis, however several obstacles must be overcome if experimentally determined substructural modal data are to be used to provide the modal information for synthesis. These problems are ; (1) selection of a synthesis method, (2) assurance of the accuracy of the modal data of substructures, (3) measurement of the rotational displacement, and (4) evaluation of the flexibility of the connecting parts. Although scalar elements (spring, mass, and dashpot) have been successfully used in synthesis based on test results, few papers have been presented that deal with the combination of plate／beam substructures, which needs the rotational displacement for synthesis.

In this project, one synthesis method was proposed for paddle structures. An unconstrained mode synthesis algorithm was adopted and the rotational displacement was calculated by differentiating the polynomial approximation over the measured lateral displacement. The availability of the method was already evaluated on two practical examples; an open isogrid panel and the solar array paddle of ETS-**V** [8].

2.1 Synthesis Method

The solar array paddle was divided into four substructures shown in the upper part of Fig. 2. The modal tests were conducted for three configurations shown in the lower part of the Fig. 2. and Fig. 3. The aim of

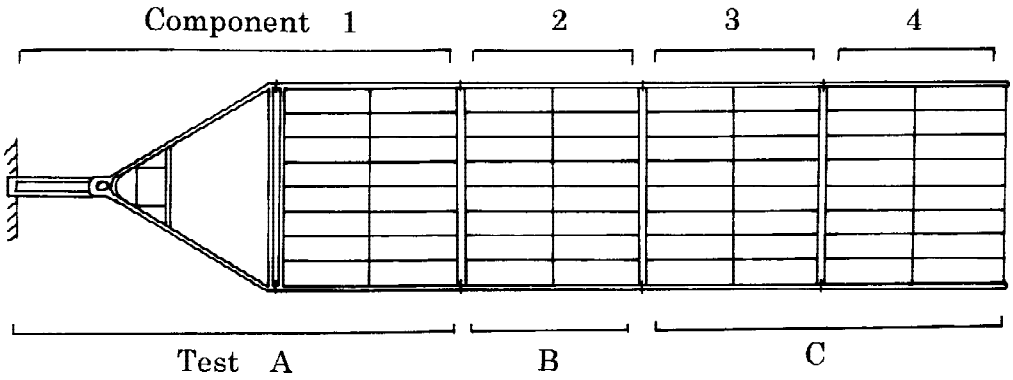

Fig. 2 Component and test configurations of the paddle

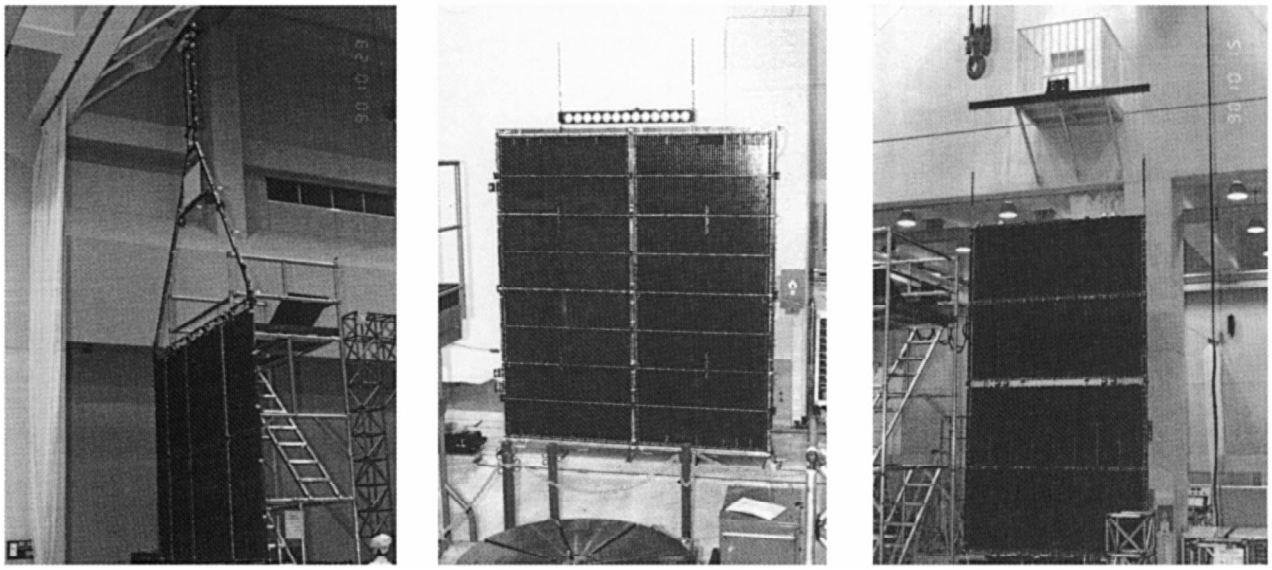

Test A Test B Test C

Fig. 3 Component Test

Test C is to obtain the spring constants for the connecting parts. The measured frequency response functions at the yoke and inner panel are shown in Fig. 4. The in-plane excitation for the flexible panel was very difficult and these frequency response functions are poor. The modes provided for the synthesis are 8 bending modes and 5 in-plane modes for Component 1, and 6 bending modes and 4 in-plane modes for Component 2, respectively. These lower mode shapes are shown in Fig. 5. These modal parameters were modified by

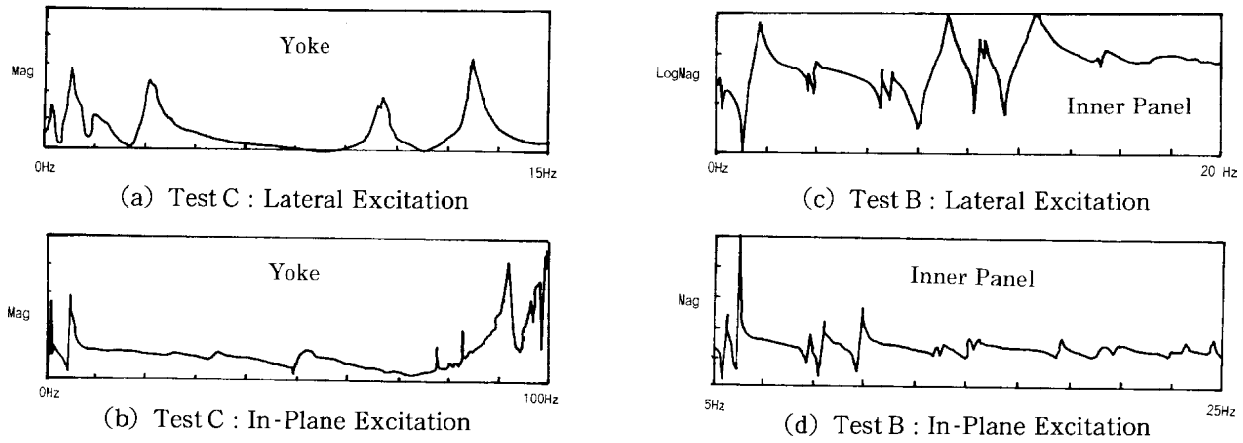

Fig. 4 Frequency Response Functions

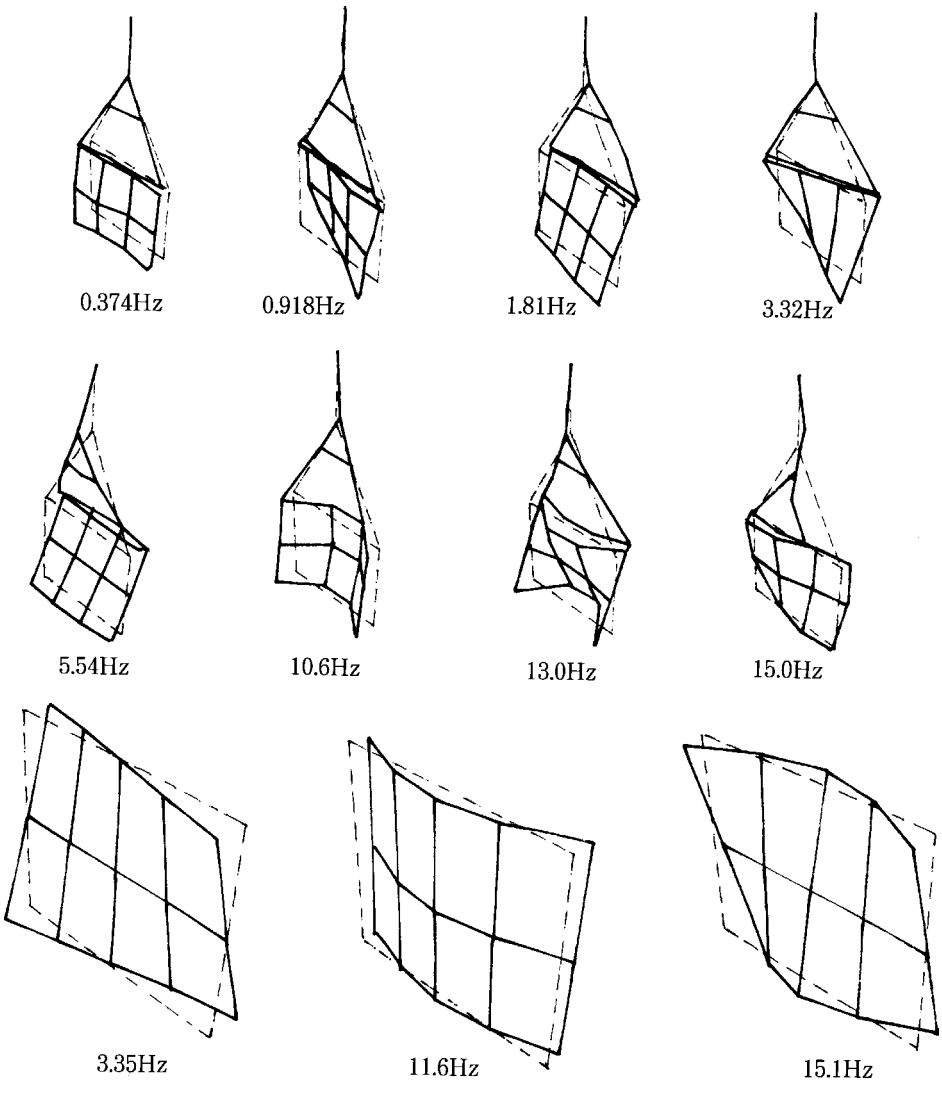

Fig. 5a Eigen Modes of Components 1 and 2 (Bending Vibration Mode)

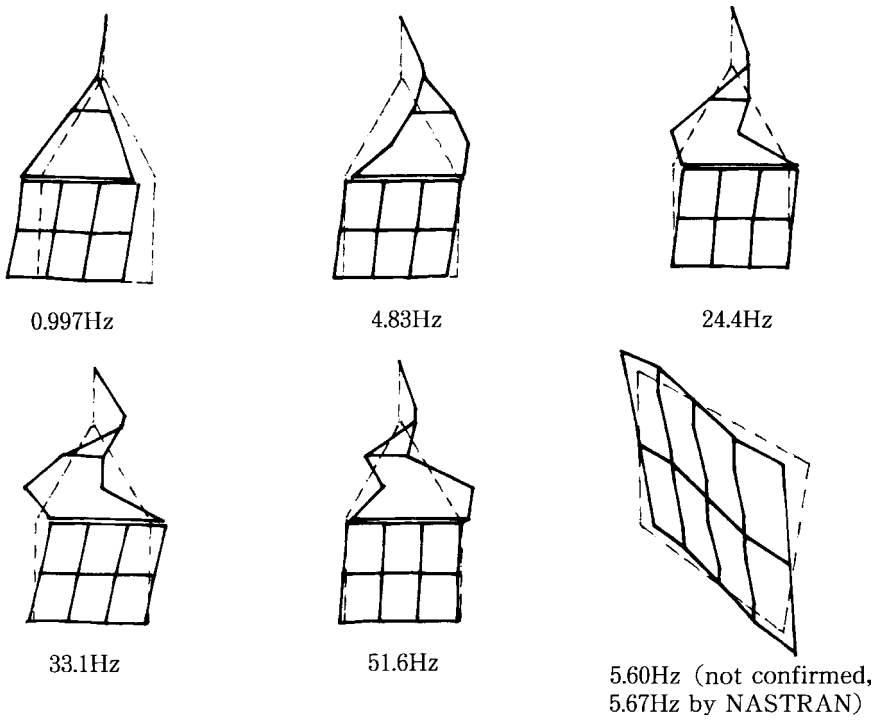

Fig. 5b Eigen Modes of Components 1 and 2 (In-Plane Vibration Mode)

the gravity and atmospheric effects by a simple order estimation using the initial finite element model.

The synthesis equation [9] is

$$\tilde{M}\ddot{q}+\tilde{K}q+\tilde{M}_c\ddot{q}+\tilde{K}_c q=0 \tag{1}$$

where the element of the vector is proportional to the contribution of motion of each substructure mode. $\tilde{M}$ and $\tilde{K}$ are diagonal matrices whose elements represent the measured modal masses and stiffnesses, respectively. $\tilde{M}_c$ and $\tilde{K}_c$ are fully populated matrices which represent the mass and stiffness of the connecting parts, and they are calculated as

$$\tilde{M}_c=\Phi^T M_c \Phi,\ \tilde{K}_c=\Phi^T \tilde{K}\Phi \tag{2}$$

where the joint matrices M_c and K_c are identified as those of an equivalent beam finite element. Matrix Φ is a mode matrix consisting of the unconstrained substructure modes. In this synthesis equation, the damping terms are not included because the measured damping ratios have only one-digit accuracy, and we can not calculate the synthesis using them.

For plate/beam structures, continuity conditions between substructures and joints have to be imposed not only on the lateral displacement but also on its derivatives (rotational displacement). This is to insure that the structure remains continuous and does not kink. At each joint, therefore, the rotational displacements must be provided, but they cannot be measured in the usual modal test. We employed polynomial approximations over the measured lateral displacement modes in order to produce the rotational displacement. The form of the polynomials employed is

$$w=c_1+c_2x+c_3y+c_4x^2+c_5xy+c_6y^2+\cdots \tag{3}$$

The order of the polynomial depends on the number of mode measuring points, and it does not exceed the forth order. The constants c_i are determined by the least-square approximation method. The rotational displacements $\partial w/\partial x$ and $\partial w/\partial y$ then can be derived directly by differentiating Eq. (3). The matrix Φ in Eq. (2) then can be enlarged by adding the terms $\partial w/\partial x$ and $\partial w/\partial y$ for each mode.

2. 2 Synthesized Results

The synthesized eigen frequencies of the paddle with a clamped-free boundary condition are listed in Table 1 comparing with those by the finite element method. The mode shapes synthesized are shown in Fig. 6. The eigen frequencies by the finite element method are modified by the synthesized results, therefore they are only for reference.

The modal parameters on-orbit can be calculated

by the standard method[10] using the synthesized modal parameters of the paddle in Table 1 and the rigid center body constants. The estimated frequencies in the orbit are listed in Table 2 with simplified mode shapes, where the body motion is exaggerated comparing with the paddle motion in order to understand the influence of the paddle motion upon the body attitude.

Table 1 Synthesized frequencies (Hz) and the modified finite element results
(OP : out of plane bending mode, IP : in-plane bending mode, TS : torsional mode, and 1, 2 denotes 1st and 2nd mode respectively)

mode	synthesis	FEM
OP 1	0.0997	0.0933
IP 1	0.245	0.250
TS 1	0.370	0.393
OP 2	0.534	0.762
TS 2	1.28	1.28
OP 3	1.43	2.055

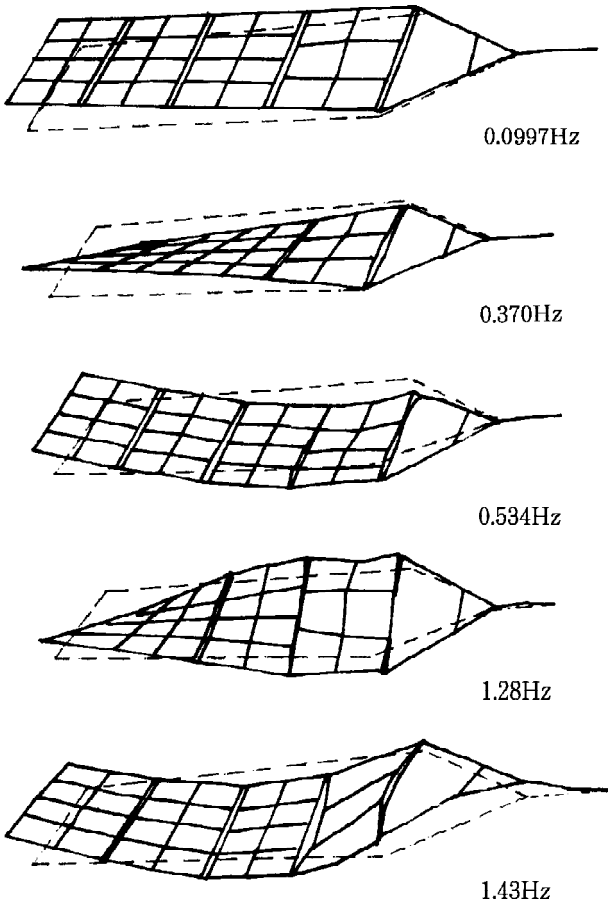

Fig. 6a Synthesized Eigen Modes of the paddle (Bending Vibration Mode)

Table 2 Pre-launch estimation of the frequency (Hz, S/and A/denotes symmetric and anti-symmetric mode respectively)

mode	synthesis	mode shape
S/OP1	0.100 Hz	
A/OP1	0.174	
S/IP1	0.252	
A/TS1	0.370	
S/TS1	0.373	
A/IP1	0.483	
S/OP2	0.539	
A/OP2	0.552	
A/TS2	1.260	
S/TS2	1.261	
S/OP3	1.434	
A/OP3	1.438	

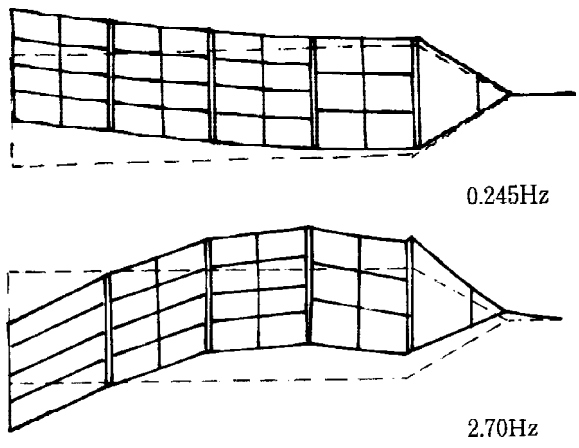

Fig. 6b Synthesized Eigen Modes of the paddle (In-Plane Vibration Mode)

2. 3 Concluding remarks

A component mode synthesis method based on experimentally determined modal parameters was applied to the solar array paddle of ETS-**VI**. The predicted parameters synthesized on the ground, which are used for the basic model for the controller design, will be compared with those obtained by the on-orbit excitation test described in the next chapter.

3. ON-ORBIT SYSTEM IDENTIFICATION

ETS-**VI** was intended to be a geosynchronous satellite with ten years life but a serious problem occurred in the liquid apogee engine. The spacecraft was finally injected into three-day regressive elliptic orbit with the period of about fourteen hours as shown in Fig. 7. FLEX experiments were performed around the apogee point, whose distance from the earth is almost the same as that of the geosynchro-nous orbit. Table 3 summarizes the contents of the identification experiments in December 1994, and in January and March 1995.

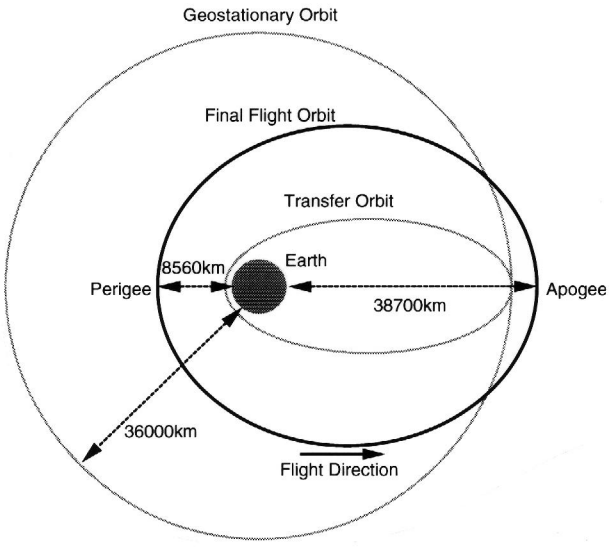

Fig. 7 ETS-**VI** transfer and final elliptic orbit

Table 3 On-orbit FLEX identification experiments on December 1994, January and March 1995

ID#	date(UT)	paddle angle	ID axis	actuator
ID# 1	12/26/94	270 [deg]	Roll (in-plane)	RCS
ID# 2	01/13/95	270 [deg]	Yaw (bending)	RCS
ID# 3	03/14/95	180 [deg]	3 axes	RCS

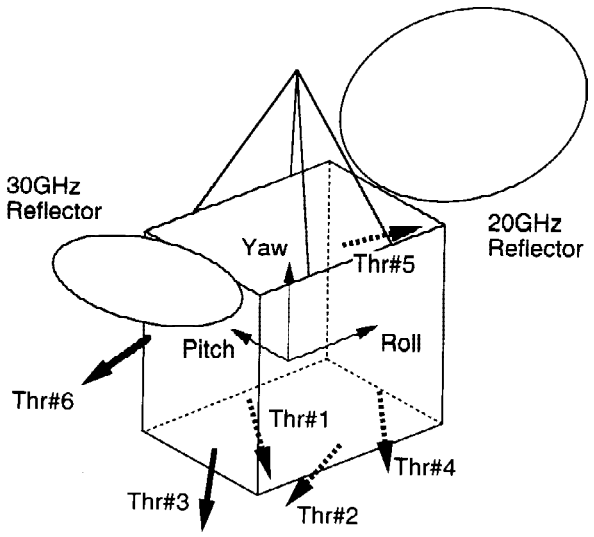

Fig. 8 RCS six thrusters location and injection direction (Thr # 1 : (+) Roll, Thr # 2 : (−) Roll, Thr # 3 : (+) Pitch, Thr # 4 : (−) Pitch, Thr # 5 : (+) Yaw, Thr # 6 : (−) Yaw)

To excite the satellite, impulse and random excitation were applied independently to the roll, pitch and yaw axes of the central body of the spacecraft by the RCS thrusters (Fig. 8). Attitude angle and attitude rate data estimated from the on-board Inertial Reference Unit (IRU), thruster drive signals and measurement data from six PACCs were packed and downloaded via S-band digital serial telemetry for the off-line analysis by several methods : the Fast Fourier Transform (FFT) and Maximum Entropy (MEM) methods in the frequency domain and the Free Decay method, Eigen system Realization Algorithm (ERA)[11], Auto Regressive model with Exogenous noise (ARX)[12], and the subspace based state space identification (SUB)[13]. Additionally Extended Kalman Filter (EKF)[14] was used to identify the parameters from the closed-loop responses during the system under attitude control. The modal parameters identified were compared with those of the pre-launch estimation and used in the synthesis of control laws which were examined in the succeeding control experiments program. In this chapter, we show the data analysis results by the methods both in the time domain and in the frequency domain.

3. 1 Method of Excitation

In the on-orbit identification experiments, the central main body of the satellite was excited on one prin-

cipal axis at a time by the 1 [N] hydrazine gas jet thrusters normally used for station keeping and attitude control. Impulse and random excitations were used to apply various kinds of methods of data analysis.

(1) Impulse Excitation

Since an ideal impulse cannot be realized by an actual gas jet thruster, the main body was disturbed by a short on-time single pulse thrusting without any attitude control. Several durations of pulse on-time to excite the vibration modes of interest were considered. The telemetry data showed the characteristics of impulse response of a rigid body with free decay. The data obtained were used in the analysis mainly in the time domain identification algorithm such as ERA and the free decay method.

(2) Random Excitation

In random excitation, the central body of the satellite was excited by randomly changing the on-off commands to a couple of thrusters in the positive and the negative directions according to maximum-length linear shift register sequence (M-sequence). The M-sequence used in the experiment is summarized in Table 4. The actual excitation pattern was slightly modified by the angular momentum control system, but it almost follows the M-sequence. Figure 8 shows the injection direction of thrusters where one thruster is injected in each direction.

3. 3 Results of the On-Orbit Experiment

The experiments have been performed holding the solar paddles at 270 or 180 degrees. In case of the 270 degree paddle angle configuration (Fig. 9 upper), it is observed that out-of-plane bending vibration is coupled with roll axis motion and in-plane bending vibration with yaw motion. On the other hand, in the 180 degree paddle angle configuration (Fig. 9 lower),

Table 4 Specification of random excitation by M-sequence noise generator

item	specification
period	1023 (10 registers)
interval	1 [sec]
excitation time	>720 [sec]
thruster on-time	80~150 [sec]

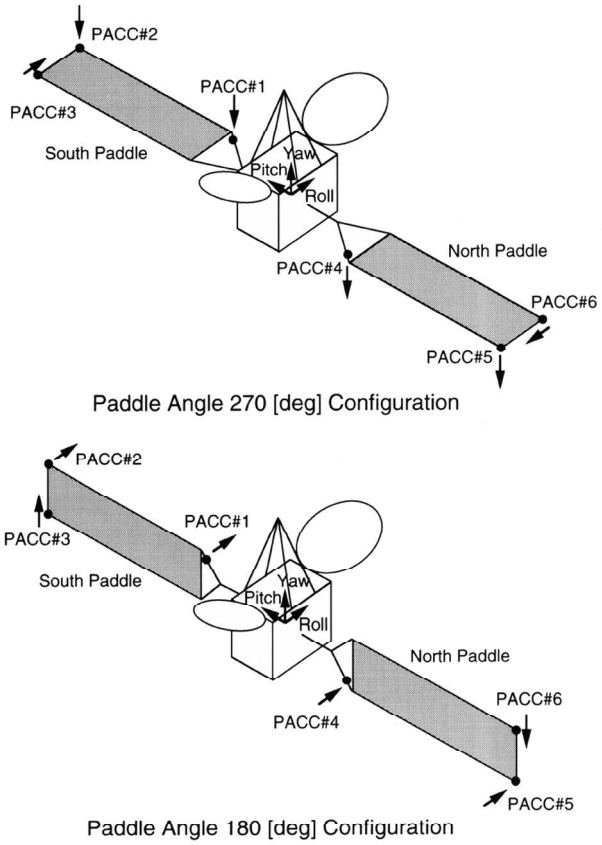

Fig. 9 PACC sensing direction and their location at paddle angle configration of 270 degrees (upper) and 180 degrees (lower)

out-of-plane vibration is coupled with yaw and in-plane with roll. However, the pitch motion is coupled only with torsional vibration in both configuration. In the identification experiments, the satellite main body attitude angles and its rates, thruster drive signals and PACC signals were sampled at a rate of 4 Hz and downlinked by 1 Hz packing on a serial digital telemetry line. Further, PACC signals were down-linked by a 24 Hz Launch Environment Monitor (LEM) line. Table 5 shows a summary of the monitored data.

Typical telemetry time response data for impulse and random excitation are shown in Fig.10 and 11 re-

Table 5 Monitored data for on-orbit identification experiments by telemetry and LEM lines

line	frequency	data	resolution
telemetry	4 [Hz]	body angle	0.0005 [deg]
		body rate	0.00032 [deg/s]
		two PACCs	1.172 [μG]
		thruster drive	0or 1
LEM	24 [Hz]	six PACCs	18.75 [μG]

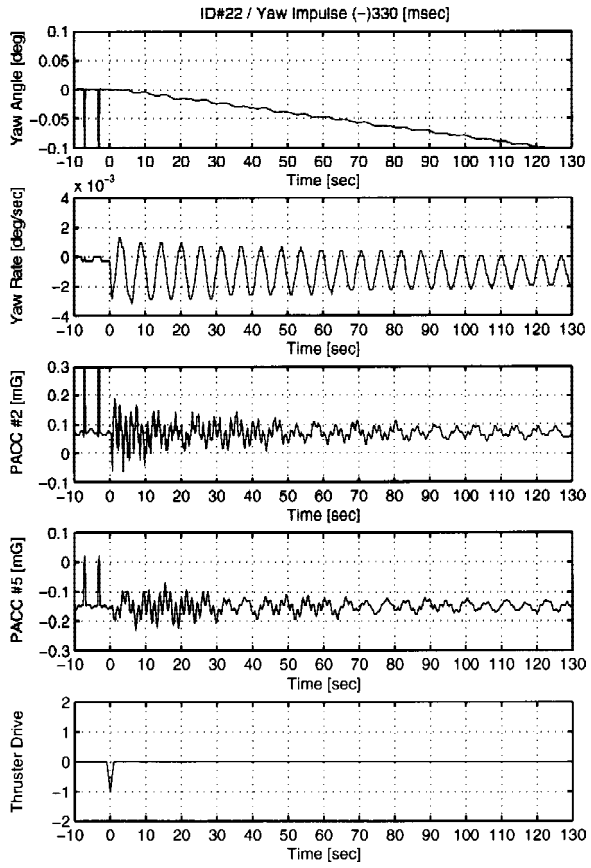

Fig. 10a Typical impulse excitation telemetry data (Case #22)

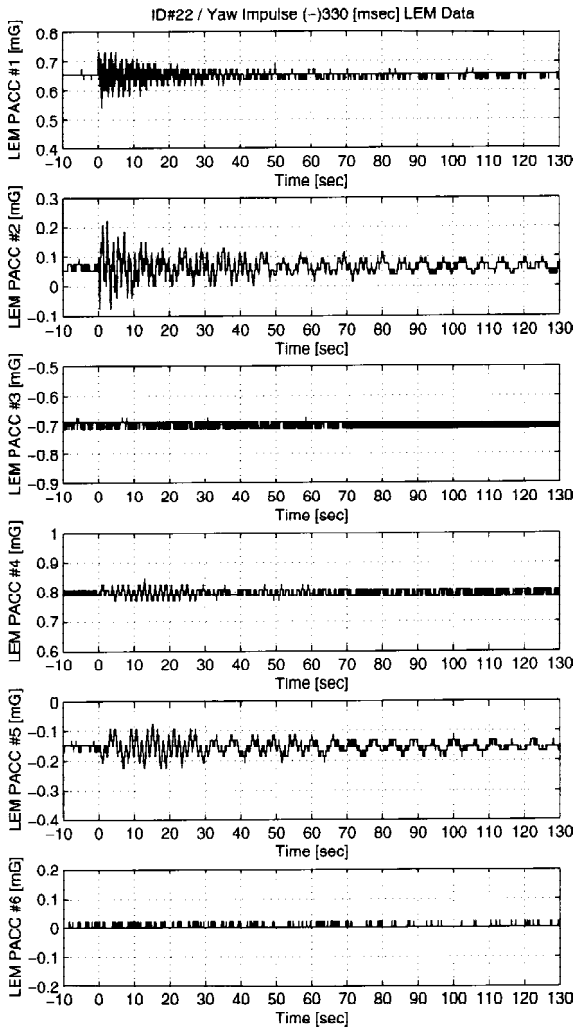

Fig. 10b Typical impulse excitation LEM PACC data (Case #22)

spectively. ERA, Free Decay method, MEM, and FFT were applied to analyze the downloaded telemetry impulse response data, and ARX, SUB, and FFT were applied to analyze the random excitation response in each axis. PACC signals on the LEM line were used for the identification of higher frequency modes since they were sampled at 24Hz and have sufficient amplitude at high frequency range modes.

Tables 6 and 7 show the on-orbit identified frequencies and damping ratios of the global system vibration modes in the 270 and 180 degree paddle angle configurations respectively. These results are again summarized comparing with the pre-launch estimation (chap.1, Table 2) in Table 8 and Figs. 12 and 13. In these figures, the damping ratios of the pre-launch estimation (FEM and CMS : Component Mode Synthesis) are assumed to be 0.5%. As for the out-of-plane bending modes, the frequencies identified by the on-orbit experiment are almost 80 - 90% of those of the pre-launch ground test and the predicted frequencies of the torsional modes also match exactly. However, a large difference exists in the frequencies of in-plane bending modes, which is mainly due to the difficulty of the ground-based in-plane excitation test. Considering the non-uniqueness of the on-orbit identified values shown in Tables 6 and 7, it can be said that the pre-launch modal estimation can predict most frequencies with at most a 10% error. Regard-ing modal damping ratios, there are large differences in the identified values depending on the method of analysis used. It is noted that the damping ratios cannot be identified from the ground analysis due to the environmental constraints and that the value of 0.5 % is widely used as a rue of thumb in engineering practice.

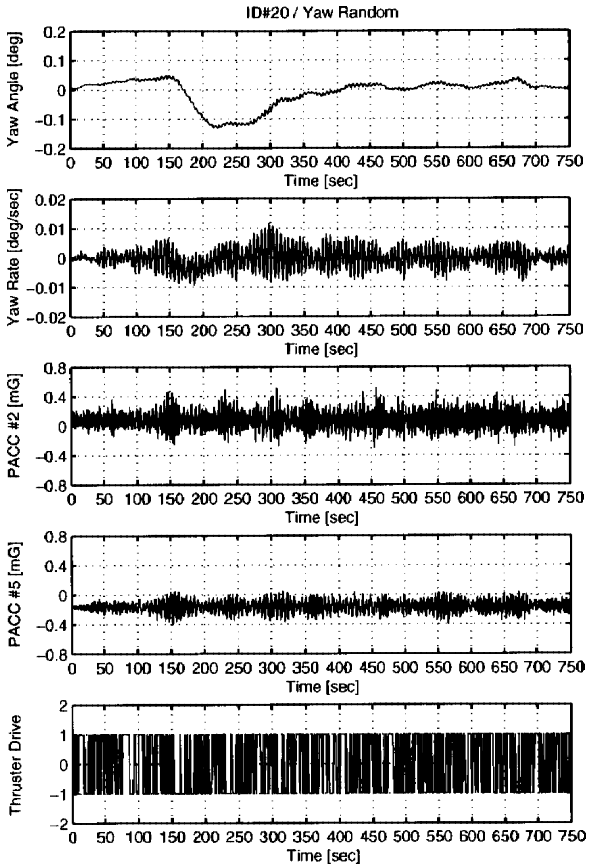

Fig. 11a Typical random excitation telemetry data (Case #20)

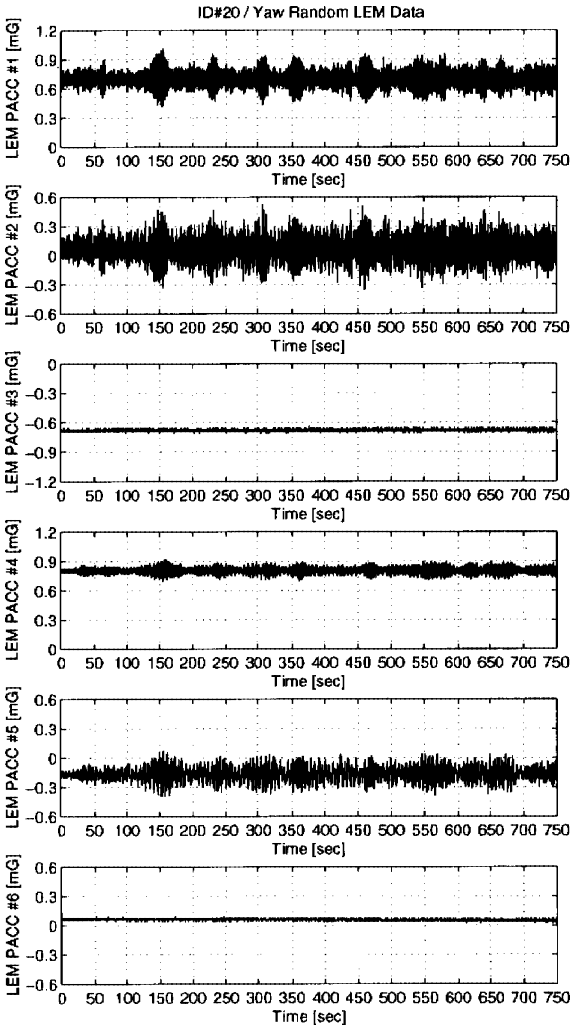

Fig. 11b Typical random excitation LEM PACC data (Case #20)

Table 6 Identified global mode frequencies [Hz] and damping ratios [%] from on-orbit experiments in the configration of 270 degrees paddle angle (S : symmetric, A : asymmetric, OP : out-of-plane bending, IP : in-plane bending, TS : Torsion)

mode	impulse				random
	Free Decay	MEM	FFT	ERA	
S/OP 1	0.0926～0.0959 1.10～1.39 %	0.125	0.109	0.0916 1.1 %	
A/OP 1	0.164～0.165 0.66～0.81 %	0.188	0.179	0.164 0.8%	0.159～0.160 1.5～1.8 %
S/IP 1	0.229～0.230 0.40～0.45 %	0.231		0.230 0.6%	0.228 0.6 %
S/TS 1		0.404		0.385	0.394～0.401 0.8 %
A/TS 1		* * *		0.398	* * *
A/IP 1	0.457～0.460 0.50～0.54 %	0.462	0.483	0.459 0.5%	0.454～0.459 0.58～0.60 %
S/OP 2		0.677	0.688	0.666 0.7%	
A/OP 2		0.686	* * *	0.683 0.7%	0.663～0.671 0.69～1.2 %
S/TS 2		1.313	1.297	1.27 0.6%	1.30 1.6 %
A/TS 2		1.406	1.375	1.34 0.7%	* * *
S/OP 3		1.641		1.64	
A/OP 3		1.781	1.750	1.66	1.78 1.0 %
S/IP 2			3.95#		3.96 0.5 %
A/IP 2			3.96#		* * *

Table 7 Identified global mode frequencies [Hz] and damping ratios [%] from on-orbit experiments in the configuration of 180 degrees paddle angle (S : symmetric, A : asymmmetric, OP : out-of-plane bending, IP : in-plane bending, TS : Torsion, paddle deploy : solar paddle ad antenna deployment)

mode	paddle deploy	impulse ERA	random ARX	random SUB
S/OP 1	0.12 10 %	0.0921 0.73 %	0.0899 2.23 %	
A/OP 1	0.17 0.3 %	0.177 0.55 %	0.174 1.39 %	0.174 1.0 %
S/IP 1	0.22 1.2 %	0.229 0.50 %		0.253 1.1 %
S/TS 1	0.39 0.4 %	0.398 0.63 %		0.384
A/TS 1	***	0.399 0.34 %	0.398 0.56 %	0.387
A/IP 1	0.14 0.8 %	0.421 0.52 %	0.420 0.55 %	0.420 0.48 %
S/OP 2		0.646 0.52 %	0.641 0.78 %	
A/OP 2		0.673 0.53 %	0.666 0.97 %	0.677 0.64 %
S/TS 2	1.24 0.5～2 %	1.267 0.45 %		
A/TS 2	***	1.278 0.65 %	1.268 0.32 %	1.215 0.24 %
S/OP 3		1.669 0.49 %	1.654 1.27 %	
A/OP 3		1.680 0.18 %	1.664 0.61 %	1.46 0.18 %
S/IP 2			4.005 0.1 %	
A/IP 2			4.059 1.62 %	

Table 8 Comparison between pre-launch synthesis and on-orbit identified mode frequencies [Hz] and damping ratios [%] in the configuration of 180 degrees paddle angle (S : symmetric, A : asymmmetric, OP : out-of-plane bending, IP : in-plane bending, TS : Torsion)

mode	pre-launch	on-orbit freq./damping
S/OP 1	0.100	0.0899～0.0921 0.7～ 2 %
A/OP 1	0.186	0.174～0.177 0.6～ 1 %
S/IP 1	0.252	0.229～0.253 0.5～ 1 %
S/TS 1	0.370	0.398～0.399 0.3～0.6 %
A/TS 1	0.373	***
A/IP 1	0.450	0.420～0.421 0.5～0.6 %
S/OP 2	0.539	0.641～0.646 0.5～0.8
A/OP 2	0.557	0.666～0.677 0.5～1
S/TS 2	1.260	1.215～1.278 0.2～0.7 %
A/TS 2	1.261	***
S/OP 3	1.434	1.654～1.669 0.5～1
A/OP 3	1.440	1.664～1.680 0.2～0.6

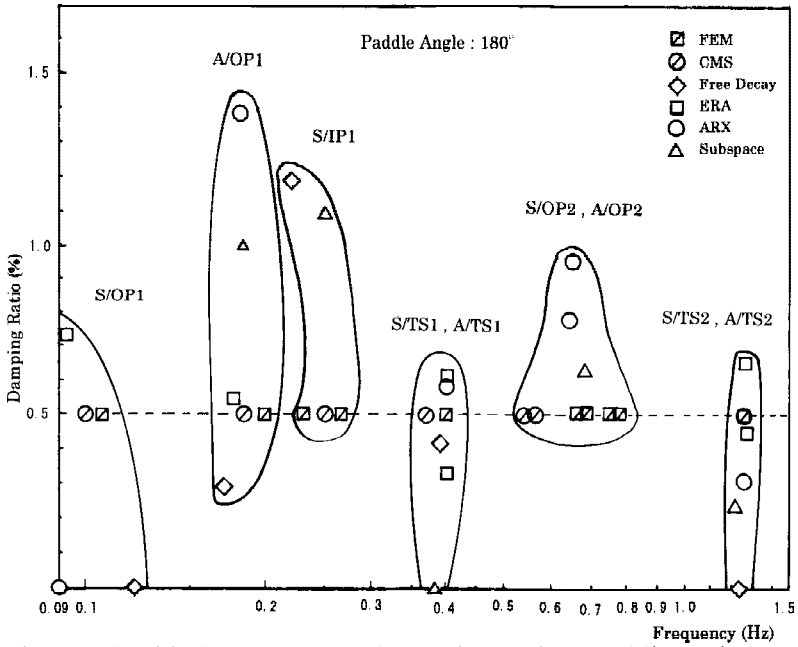

Fig. 12 Identified Frequency and Damping Ratio at Paddle angle 180°

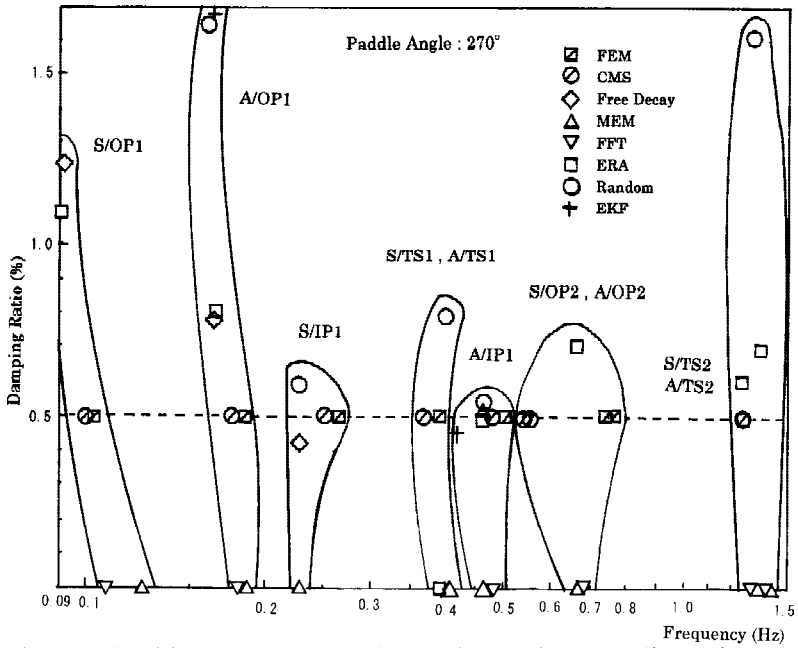

Fig. 13 Identified Frequency and Damping Ratio at Paddle angle 270°

3. 4 Concluding Remarks

The results of ETS-VI on-orbit system parameter identification experiments are summarized in this chapter. Impulse and random excitation experiments were performed more than twenty times for three days and noise-free clear data were obtained as expected. Various identification methods were applied to the flight data and compared with each other. Additionally, the results were compared with the pre-launch estimate to evaluate the accuracy of ground analysis. Identified precise model was used to the attitude control system design. These results are considered to be significant for the future large space structure modeling technologies on the view points of pre-launch ground analysis and on-orbit identification.

4. ATTITUDE CONTROL EXPERIMENT

4. 1 Control System

The attitude control experiments were carried out for 16 days from December 1994 to July 1995. In this period, more than ten control algorithms were exam-

ined.

The experiment made use of Attitude Control Subsystem (ACS) of ETS-**VI** and six accelerometers (PACC) mounted on the paddles. The attitude angles and rates are precisely determined by Earth Sensors Assembly (ESA), Inertial Reference Unit (IRU) and Rate Integrated Gyro Assembly (RIGA). The primary actuators are four reaction wheels (RW) located in skew-configuration, and Reaction Control System (RCS) was optionally used. The on-board control algorithms for the experiment were remotely loaded to RAM (Random Access Memory) area of the ACE (Attitude Control Electronics) from the ground station, and were executed by commands. During the closed-loop control experiment, attitude angles, attitude rates, control signals, and vibration acceleration of PACCs were monitored. Then these data were transmitted to EWS (Engineering Work Station) for the further analysis and evaluation.

4. 2 Control Laws

In order to design Reduced Order Controller (ROC), we make Reduced Order Model (ROM) from the Full Order Model (FOM) of the design model. By considering modal frequencies, the controller sampling rate, and phase delay, we made ROM for OP (Out of Plane bending mode), IP (In-Plane bending mode) and TS (TorSional mode). The ROM of OP consists of rigid mode and 1st vibration mode. The IP 1st mode is optionally included in ROM, since its frequency is critical for implementing reliable controller. On the other hand, the effect of vibration is negligibly small for TS. Therefore TS motion can be regarded as a rigid body.

Over ten control algorithms were applied. These are grouped into the following six categories.

(1) I-PD : Controller is designed by frequency domain model matching method to attain the assigned lower-frequency control performance and robust stability[15].

(2) LQG : By using frequency dependent Linear Quadratic (LQ) cost functional, the obtained optimal LQ gain has the high roll-off rate in the high-frequency range, which makes the closed-loop system robust against residual modes[16].

(3) H^{∞} : Mixed-sensitivity problem formulation is employed with the aid of stability degree assignment, or collocated Direct Velocity FeedBack (DVFB)[16].

(4) H^{∞} and Two-DOF : In order to improve the tracking property, H^{∞} servo problem is solved. Additionally two degree-of-freedom controller is constructed to follow the assigned response, accurately[17].

(5) H^{∞} : Loop-shaping capability of normalized coprime factorization method is applied to achieve both the high control performance in the low-frequency range and the robust property in the high-frequency[18].

(6) LAC／HAC : The modal damping of the panel vibration is enhanced by using acceleration signals from six PACCs attached at solar panels. This is non-collocated law authority control[19].

All controllers were designed using linear controller synthesis CAD. Then, they are converted to the discrete time controllers. For implementation, they are further quantized by PRM (Pseudo Rate Modulator) when RCS is used as the control actuator. When RW is used, the three-axis control command is transformed to four skew RW command according to the distribution law.

As a design example, the LQG for OP (left) controllers are shown by Bode plots of the loop-transfer function (solid line) and the transfer function of controller (dotted line) in Fig.14. The controller is described by two-point (attitude and rate) one-output (torque) transfer function. The OP controller stabi-

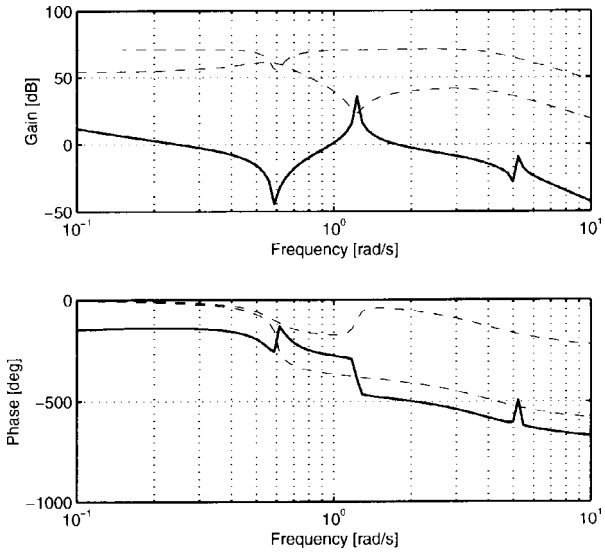

Fig. 14 LQG design result of OP controller ; Bode plots of loop transfer function (solid) and controller transfer function (broken)

lizes the first mode by the phase margin and the second mode by the gain margin. The former is the phase stabilization and the latter is the gain stabilization. By IP controller, all the vibration modes are gain stabilized. Therefore, the cut-off frequency of OP controller is higher than that of IP. Design results of IP and TS controller are omitted in this paper.

4. 3 Pre-Launch Evaluation

In the controller synthesis phase, the sensitivity to the parameter uncertainties of the closed-loop system was evaluated by simulating its responses from various aspects. Based on the results, controller parameters were tuned repeatedly. This is the evaluation in the world of the linear time imvariant system. However many kinds of unmodelled dynamics and complicate computer logics, which might violate the stability or the performance of the closed-loop system, may reside in the actual spacecraft system. In order to cope with the anxiety, we have made following ground-based pre-launch evaluations, before the on-orbit experiment.

(1) Air／Table experiment : Digital control experiment was performed by using a ETS-**VI** miniature model mounted on the table floated by air bear-ing[20].

(2) Static Closed-Loop Test (SCLT) : A setup of the ETS-**VI** dynamics computer simulator linked to the ACE／EM (Engineering Model) was used to examine the on-board control logics[21].

(3) Simulation : Numerical simulation was made to evaluate the performance of controller in the real world. It computes linear modal equation and critical components of ETS-**VI**, such as Attitude Determi-nation Logic, PRM, RW Drive Electronics (WDE)[22].

(4) Simulation : Numerical simulation was made to evaluate on-board software of machine language. The simulator has the capability of ACE／CPU emulation.

Each evaluation has played its own role in each development phase. A lot of bugs and defects of control laws have been fixed through them.

4. 4 Results of the Control Experiments

The control experiments were performed by holding the panel rotation at the angles of 270 degrees (or 180 degrees according to the experiment date), in order to avoid the disturbance torque caused by PDE (Paddle Drive Electronics). The initialization of the system and wheel unloading were made during the bus controller was in operation. Then the control logic was changed to the law of the experiment from that of bus control. We obtained step response to the attitude command and impulse response to the disturbance torque to evaluate the controller performance.

Fig. 15 is the experimental results of LQG controller using RCS as control actuators. From top to bottom, the time responses of roll, pitch, yaw angles, roll-rate, pitch-rate, and yaw-rate are shown. The experiment is operated by the following sequence. First, the attitude commands of $+0.05°$, $-0.05°$, and $0°$ were sequentially added to the roll control system. The same operations were made for pitch and yaw. Then the pulse disturbance torque of the width of **1** sec was

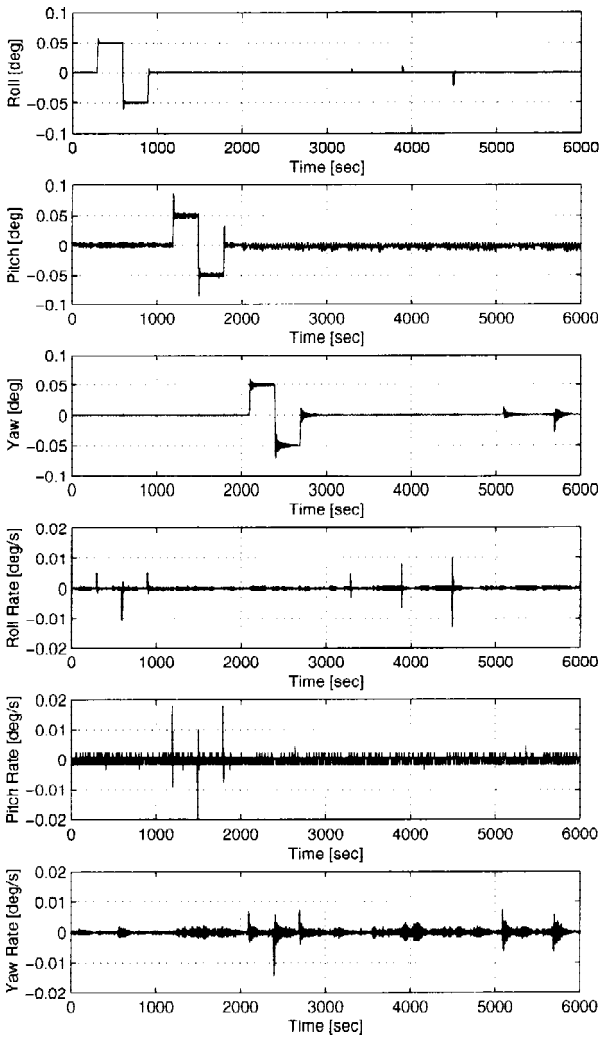

Fig. 15 Experimental results of LQG/RCS ; from top to bottom, roll, pitch, yaw angle in [deg] and roll rate, pitch rate, yaw rate in [deg/s]

applied to +roll direction and that of 2 second to − roll direction by RCS. The same disturbance responses were obtained for yaw. The experiment was performed in the configuration of 270 degree paddle angle in January 1995. In this case, the OP controller controlled roll attitude and IP controller controlled yaw attitude. The robust stability and the disturbance rejection capability were verified. Additionally, by comparing roll, yaw responses, it was observed that the wide-range OP controller is more effective than the narrow-range IP controller in the disturbance rejection capability.

In Fig. 16, the step and the impulse responses of roll, roll-rate, roll-torque command of the experiment result is shown (thick line), compared with the responses estimated at the design phase (thin line). And the closed-loop frequency response of roll angle calculated from the power spectrum density of the impulse responses are shown in Fig. 17 (solid line) compared with the amplitude of the designed closed-loop transfer function (thin line). It is noted that the vibration mode is sufficiently suppressed despite the parameter error.

4. 5 Post-Flight Analysis

From the analysis of the flight data, it turned out that many controllers have behaved just as designed. In some cases, however, expected performances have not been achieved. In order to clarify the reasons, we made the following evaluation.

(1) The closed-loop system was identified and verified from the closed-loop impulse response in both the frequency and the time domain[18].

(2) The closed-loop responses of controllers applied to evaluation model was computed and compared with flight data[16][17].

(3) The effects of other uncertainties such as RCS torque level were investigated.

In addition, we have made controller reconfiguration experiment by retuning controller based on the on-orbit identified modal parameters. The retuned controller has successfully stabilized the 1st IP bending mode which was originally destabilized by the controller designed based on the prelaunch model.

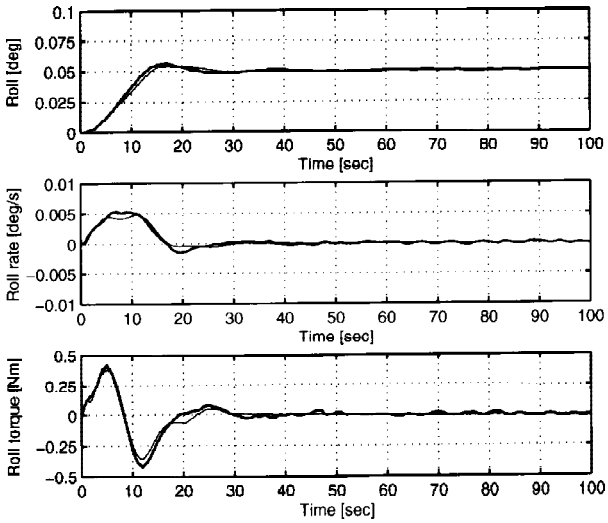

Fig. 16a Time response of LQG (OP) controller for step command ; experiment (thick) and design (thin)

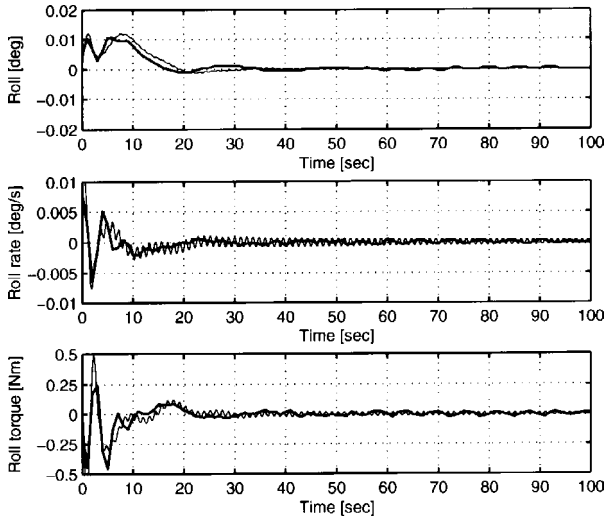

Fig. 16b Time response of LQG (OP) controller for impulse command ; experiment (thick) and design (thin)

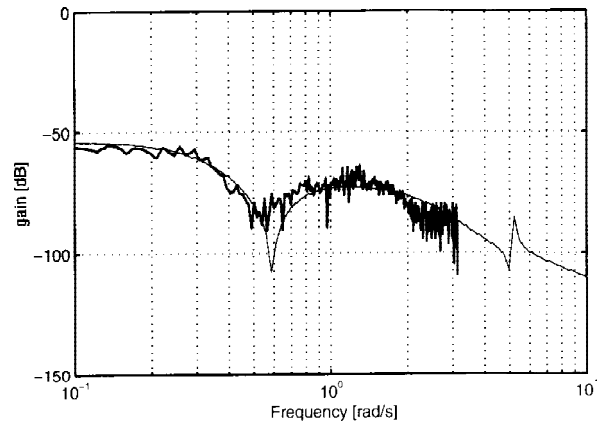

Fig. 17 Frequency response of controller LQG (OP) experiment (thick) and design (thin)

4. 6 Concluding Remarks

In summary, the followings are concluded. The important role of robust controller was, as expected, proved by the experiment. This is the principal result of this chapter. Additionally, we have shown that on-orbit identification is feasible and it can provide more accurate model. Therefore, it is promising to re-tune the controller parameters in orbit for enhancing the control performance.

5. CONCLUSIONS

The methods of pre-launch modeling, on-orbit modal parameter identification and controller synthesis are described and the experimental results are shown and discussed.

For pre-launch model, a component mode synthesis technique using measured modal data was applied to the flexible solar array paddle. After the launch, the spacecraft was excited by the reaction control system, and the modal parameters were identified based on the telemetry data of the on-board accelerometers. The attitude controllers were designed based on the pre-launch model and executed in orbit, of which some controllers were re-tuned based on the on-orbit identification model.

Through the on-orbit experiment, we have evaluated the pre-launch modeling method, the on-orbit identification method and the feasibility of the robust control.

Acknowledgement

This experiment was carried out jointly by National Aerospace Laboratory (NAL) and National Space Development Agency (NASDA) supported by Toshiba Corporation and Mitsubishi Electric Corporation. The authors wish to gratefully acknowledge the engineers and researchers involved in this project.

REFERENCES

1) Garg, S. C. and Hughes, P. C. ; Flight Results on Structural Dynamics from Hermes, J. Spacecraft, Vol. 16, No. 2 (1979) pp. 81-87.

2) Schock, R. W. ; Solar Array Flight Dynamics Experiment, Proc. of Workshop on Structural Dynamics and Control Interaction of Flexible Structures, held at MSFC, Alabama (1986／4) pp. 487-504.

3) Grocott, S., How, J., Miller, D., MacMartin, D., and Liu, K., ; Robust Control Design and Implementation on the Middeck Active Control Experiment, J. of Guidance, Control, and Dynamics, Vol. 17, No. 6 (1994) pp. 1163 - 1170.

4) Bukley, A. P. ; Hubble Space Telescope Pointing Control System Design Improvement Study Results, J. of Guidance, Control, and Dynamics, Vol. 18, No. 2 (1995) pp. 194 - 199.

5) NAL - NASDA ; On - Orbit Flexible Structure Control Experiment of Engineering Test Satellite-, First study report of NAL-NASDA joint work, National Aerospace Laboratory and National Space Development Agency, (1987／3) (in Japa-nese).

6) NAL-NASDA ; On-Orbit Flexible Structure Control Experiment of Engineering Test Satellite-, Second report of NAL-NASDA joint work, National Aerospace Laboratory and National Space Development Agency (1989／3) (in Japa-nese).

7) NAL-NASDA ; On-Orbit Flexible Structure Control Experiment of Engineering Test Satellite-**VI**, Final report of NAL-NASDA joint work, National Aerospace Laboratory and National Space Development Agency (1996／3) (in Japa-nese).

8) Komatsu, K., Sano, M., Kai, T.,Tsujihaha, A., and Mitsuma, H. ; Experimental Modal Analysis for Dynamic Models of Spacecraft, J. of Guidance, Control, and Dynamics, Vol. 14, No.3 (1991) pp. 686-688.

9) Ewins, D. J. ; Modal Testing : Theory and Practice, Research Studies Press LTD., Letchworth (1984) pp. 245-246.

10) Likins, P. W. ; Dynamics and Control of Flexible Space Vehicles, NASA TR 32-1329 (1970).

11) Yamaguchi, I., Kida, T., and Kasai, T.; Experimental Demonstration of LSS System Identi-fication by Eigensystem Realization Algo-rithm, Proc. of 1995 American Control Conference (1995) pp. 407-411.

12) Ishikawa, S., Yamada, K., Yamaguchi, I., Chida, Y., and Adachi, S. ; ETS-**VI** On-orbit Parameter Estimation by Random Excitation, Proc. of Astrodyna-mics Symposium (1995).

13) Adachi, S., Yamaguchi, I., Kida, T., and Sekiguchi, T. ; ETS-**VI** On-Orbit Identification Experiment (Part 4) - Subspace Method-, Proceedings of 39th Space Sciences and Technology Conference, (in Japanese) (1995) pp. 495-496.

14) Kasai, T., Komatsu, K., and Sano, M. ; Modal Para-

meter Identification of Controlled Flexible Structures, AIAA J. of Guidance, Control and Dynamics, Vol. 20, No. 2 (1997) pp. 184-186 .

15) Chida, Y., Yamaguchi, Y., Soga, H., Kida, T., Yamaguchi, I., and Sekiguchi, T. ; Attitude Control Experiment on Orbit Using ETS- **VI** , submitted to 35th CDC, Kobe, (1996) pp. 486-488.

16) Kida, T., Yamaguchi, I., Chida, Y. and Sekiguchi, T. ; On-orbit Robust Control Experiment of Flexi-ble Spacecraft ETS-**VI**, AIAA Paper 96-3843, AIAA Guidance, Navigation and Control Conference, SanDiego (1996).

17) Chida, Y., Yamaguchi, Y., Soga, H., Kida, T., Yamaguchi, I., and Ishikawa, S. ; On - Orbit Attitude Control Experiments of ETS- **VI** , ISTS ／ IAS 96-C-66p, Gifu (1996).

18) Kashiwase, T., Yamada, K., Awa, Y., Sekiguchi, T., and Kida, T. ; On-Orbit Experiments of Frequency-Shaped H∞ Control for Flexible Space Structures, ISTS／IAS 96 - C - 67p, Gifu (1996).

19) Ichikawa, S., Kashiwase, T., Miyazaki, K., and Kida, T. ; ETS-**VI** Attitude Control Experiments (in Japanese), SICE Guidance Control Symposium, Nagano (1995).

20) Mine, M., Soga, H., Kida, T., Yamaguchi, I., Iino, Y. and Chida, Y. ; ETS- **VI** Attitude Control Experiments on Orbit with Flexible Structures, International Symposium on Theory of Machines and Mechanics, Nagoya (1992) pp. 775-780.

21) Kida, T. ; Large Flexible Spacecraft Control and Its On - Orbit Experiment, NAL Research Progress (1994) pp. 64 - 65.

22) Yamaguchi, I. and Kida, T. ; Dynamical Model and Numerical Simulations for Engineering Test Satellite-, NAL Technical Reports TR-1239 (1994).

22) Yamaguchi, I and Kida, T. ; Dynamical Model and Numerical Simulations for Engineering Test Satellite-**VI**, NAL Technical Reports TR-1239 (1994).